Army Research Laboratory
Aberdeen Proving Ground, MD 21005-5066

ARL-TR-2046 **September 1999**

Calculating the Chemical Compositions of Plasmas Generated by an Ablating-Capillary Arc

M. J. McQuaid and M. J. Nusca
Weapons and Materials Research Directorate, ARL

Abstract

The NASA-Lewis computer program for the calculation of complex chemical equilibrium compositions (CEA) is proposed as a means of characterizing the compositions of plasmas generated via an ablating-capillary arc. Results obtained with CEA are compared to those obtained with a Saha equation-based (SE) model with a limited reaction product set. Case studies conducted at temperatures from 5,000 to 20,000 K and pressures from 10 to 200 bar indicate that CEA warrants consideration for use in modeling such plasmas.

Acknowledgments

The authors would like to thank Dr. John Powell for providing us with his program for simulating an ablating-capillary arc discharge and for many helpful discussions regarding the physics on which the program is based. Dr. A. Kotlar helped us to get started using the NASA-Lewis computer program for the calculation of complex chemical equilibrium compositions (CEA) and provided insight into its workings.

INTENTIONALLY LEFT BLANK.

Table of Contents

INTENTIONALLY LEFT BLANK.

List of Figures

INTENTIONALLY LEFT BLANK.

List of Tables

INTENTIONALLY LEFT BLANK.

1. Introduction

Ablating-capillary arcs are a means of converting electrical energy into a form suitable for the ignition of propulsion charges in large-caliber gun systems [1]. In ignition systems that utilize this approach, electrical energy stored in a pulse-forming network (PFN) is initially discharged via a thin metallic wire strung through the capillary. The initial discharge explodes the wire, "instantaneously" producing an ionized (plasma) gas into which the PFN continues to dump energy. Ablation of material from the capillary wall, which is generally attributed to (and modeled as) a radiation driven process [2], serves to sustain the arc by replenishing gas that exits the capillary. The overall process produces a "dense" (10^{23}–10^{26} m^{-3}), "low-temperature" (10,000–30,000 K) plasma whose composition is primarily derived from decomposed capillary material [2]. This fluid subsequently flows into the propellant bed and ignites it (directly).

Ablating-capillary arcs were one of the first electrothermal-chemical (ETC) ignition concepts to be investigated, and experimentally observed attributes—including short, reproducible ignition delays [1], propellant burn rate enhancement [3], and "temperature compensation" [4, 5]—have been bases for believing that ETC-based concepts are capable of substantially enhancing the ballistic performance (projectile muzzle velocity or kinetic energy) of currently fielded weapon systems [1]. Unfortunately, the mechanisms that underlie the experimental observations have yet to be established, making the design of a fieldable ignition system an elusive goal. This report summarizes part of an effort to develop a state-of-the-art computational fluid dynamics (CFD) model of the plasma-propellant interactions attending ablating-capillary arc-based ignition [6, 7]. It is considered that such a model will serve to elucidate the mechanisms by which this ignition concept yields its promise. Moreover, it is considered that mechanisms underlying ablating-capillary arc-based ignition will be relevant to (and can be exploited for) the development of other ETC-based ignition concepts.

The dynamics of the generation and evolution of the fluid produced by an ablating-capillary arc are highly complex, and a detailed characterization of the process requires cross-disciplinary expertise in plasma physics, fluid dynamics, and chemical kinetics. The work presented in this

report concerns the characterization of the chemical composition of the effluent from an ablating-capillary arc—an issue typically addressed by reference to plasma physics concepts and theories. Of particular importance to the characterization of an ablating-capillary arc is the concept of local thermodynamic equilibrium (LTE) (e.g., see Griem [8]). The concept of LTE is relevant to systems in which collision-induced transitions and reactions are more frequent than radiative transitions. If, in addition, there is microreversibility between the collision processes, the steady-state solution of the rate equations yields population distributions that are the same as those of a system in complete thermodynamic equilibrium (where the radiation temperature and the temperature of the reacting particles are equal). Thus, when LTE can be assumed, Boltzmann distributions, Saha equations, and the mass action law remain valid for describing the relative populations of reacting particles even though the radiation distribution may deviate from a Planck function. These formulae, together with reaction product rovibronic energy level data, provide a "microscopic" description of the plasma that allows the population distributions of all species—neutrals as well as ions—to be calculated based on knowledge of total "heavy nucleus" densities and temperature (alone). (A model based on these formulae is subsequently referred to as a Saha equation [SE] model.) This "reduction" of the problem greatly facilitates the characterization of a plasma's chemical composition.

The plasmas produced by an ablating capillary arc are relatively dense, making the assumption of LTE appropriate for such systems, and SE models are a standard means for characterizing their chemical compositions. For complex systems, the main effort involved in developing an SE model for a given application is the building of an appropriate reaction product rovibronic energy level database. This is not too difficult if only monatomic species need to be considered. However, at the low end of temperatures (10,000 K) relevant to arc discharge processes, it is expected that the density of polyatomic species will be significant [9]. Since the development of the reaction product database needed to model such systems would be an extremely arduous and time-consuming task, we decided to determine if the NASA-Lewis computer program for the calculation of complex chemical equilibrium compositions (CEA) could be employed for this purpose. CEA, whose origins date to 1967, is a well-established tool within the combustion community (where it is often simply referred to as the NASA-Lewis

code). Details of the code may be found in references by McBride and Gordon [10, 11]. Briefly, the program permits (among other things) the calculation of chemical equilibrium compositions for assigned thermodynamic states. It does so based on a "macroscopic" mathematical approach—Gibb's free-energy minimization. One of the attractions of CEA is the extensive library of reaction product thermodynamic data (THERMO.INP) that has been developed for use with it. Information on more than 1,300 species is included in the library in our possession. Originally developed for characterizing systems at temperatures up to 6,000 K, in recent years the library has been expanded to allow for the calculation of property data of selected species at temperatures up to 20,000 K. Among the species with properties derivable to 20,000 K are all of the neutral and +1 ions of the atoms and diatoms that can be formed in a gas containing C, H, N, and O nuclei. This expansion of the library raised the possibility of using CEA to characterize ablating-capillary arc operation in this temperature regime, and thus avoid significant model development effort.

With respect to calculating the chemical compositions of plasmas, the shortcoming of CEA is that it doesn't include a correction to the Gibb's free energy (calculation) that accounts for the influence of interactions between charged particles. These interactions, which are generically referred to in this report as "Coulomb interactions," will act to lower the ionization potential of plasma constituents and (otherwise) influence constituent thermodynamic properties. (That is, the thermodynamic properties of a plasma constituent will depend on the presence and density of other heavy-nuclei in the plasma.) Therefore, it is not clear how useful CEA will be in characterizing the composition of plasmas generated by an ablating-capillary arc.

To determine if CEA can be used to characterize the composition of the effluent from an ablating-capillary arc, we compare the compositions computed by CEA with those of an SE model that accounts for Coulomb interactions, but employs a reaction product set with only monatomic species. The SE model employed in this study is the same as that employed in Powell and Zielinski's (PZ) model of an ablating-capillary arc [2], their model having been employed as the "source term" for a previous CFD model of the expansion of a plasma jet into a combustion chamber [7]. The comparison is conducted for plasmas formed from the decomposition of polyethylene [$(C_2H_4)_n$], a material that has been extensively used and studied

in this application [2]. Results are presented for plasma temperatures in the range from 5,000 to 20,000 K and pressures in the range from 10 to 200 bar. This regime is relevant to the ignition phase of an interior ballistic cycle. In addition, from a modeling standpoint, it is a transitional regime, with CEA expected to yield better estimates for lower temperatures and pressures and the SE model expected to provide better estimates for higher temperatures and pressures. Thus, beyond addressing the issue of employing CEA to characterize the chemical composition of an ablating capillary arc, the study is instructive as to the use of an SE model for characterizing low-temperature plasmas when the reaction product data set employed with the model includes only monatomic species.

2. Model Considerations

2.1 The SE Model. For a plasma in LTE, the relative concentrations of the $(j+1)^{th}$ and j^{th} ionization states of the i^{th} atomic nucleus at a temperature (T) may be estimated via the Saha equation [8],

$$\frac{n_{i,j+1}n_e}{n_{i,j}} = \frac{2Z_{i,j+1}(T)}{Z_{i,j}(T)}\left(\frac{2\pi m_e k_b T}{h^2}\right)^{3/2}\exp\left(\frac{-(E^{\infty}_{i,j}-\Delta E^{\infty}_{i,j})}{k_b T}\right), \tag{1}$$

where $n_{i,j}$ is the number density of specie (i,j), $E^{\infty}_{i,j}$ is its "isolated state" ionization potential, and $\Delta E^{\infty}_{i,j}$ is the reduction of $E^{\infty}_{i,j}$ due to Coulomb interactions. Other parameters in the equation are the electron number density (n_e), the partition function [$Z_{i,j}(T)$], the rest mass of an electron (m_e), Planck's constant (h), and Boltzmann's constant (k_b). For monatomic species, the partition function is a function of a specie's electronic energy level structure only and is computed using

$$Z_{i,j}(T) = \sum_k g_{i,j,k}\exp\left(\frac{-E^k_{i,j}}{k_b T}\right), \tag{2}$$

where $g_{i,j,k}$ is the statistical weight (factor) for energy level $E^k_{i,j}$.

In applying equation (1) for the computation of chemical compositions, the estimations of $\Delta E_{i,j}^{\infty}$ and $Z_{i,j}(T)$ are issues. The parameter $\Delta E_{i,j}^{\infty}$ reflects the fact that Coulomb interactions allow the electrons of an atom or ion to escape the central force field of the nucleus at energies less than the ionization potential of an isolated atom or ion. Thus, the ratio of $(j+1)^{th}$ to j^{th} ionization states for the i^{th} nucleus in a plasma will be higher than that estimated assuming that charged constituents do not "interact." For estimating $\Delta E_{i,j}^{\infty}$, we chose to follow PZ [2] and calculate this parameter based on the model proposed by Eberling and Sandig [12],

$$\Delta E_{i,j}^{\infty} = \frac{je^2}{4\pi\varepsilon_o(\lambda_D + \Lambda/8)}, \tag{3}$$

where e is the electronic charge, ε_o is the permittivity of free space, Λ is the DeBroglie wavelength,

$$\Lambda = \frac{h}{(2\pi m_e k_b T)^{\frac{1}{2}}}, \tag{4}$$

and λ_D is the Debye length,

$$\lambda_D = \left(\frac{\varepsilon_o k_b T}{n_e e^2 (1+z)} \right)^{1/2}. \tag{5}$$

The parameter z in equation (5) represents the effective charge on an ion, this parameter being computed via the equation

$$z = \frac{\sum_i \sum_j j^2 n_i x_{i,j}}{\sum_i \sum_j j n_i x_{i,j}}, \tag{6}$$

where $x_{i,j}$ is the ratio

$$x_{i,j} = \frac{n_{i,j}}{\sum_j n_{i,j}}. \tag{7}$$

It is worth noting that, in this approach, $\Delta E_{i,j}^{\infty}$ increases nearly in proportion to $n_e^{1/2}$ while decreasing in proportion to $T^{1/2}$.

The difficulty of computing $Z_{i,j}(T)$ can be appreciated by noting that the partition function becomes infinite unless the summation is truncated. (Near the series limit, the exponential term remains nearly constant while the statistical weight increases with principle quantum number [n].) To address this difficulty, it is typically assumed that Coulomb interactions have a negligible effect on the energy level structure of individual constituents and the reduction in ionization potential is employed as a basis for limiting the summation in equation (2) to energy levels [8]

$$E_{i,j}^{\max} \leq E_{i,j}^{\infty} - \Delta E_{i,j}^{\infty} \tag{8}$$

With this set of assumptions, calculation of $Z_{i,j}(T)$ simply becomes a matter of identifying all of the energy levels for a constituent up to this limit. Identification of these levels can be accomplished by reference to experimentally based data tables and/or through computational techniques. We have relied on both approaches, the details of which are given in Appendix A.

Estimates of chemical composition follow from the solution of equations (1)–(8), which are identical to those employed by the PZ model for simulating an ablating-polyethylene capillary arc [2]. For the calculation of the partition functions in this study, however, we include higher energy levels for C, C^+, C^{++}, and H. In the case of carbon—the only case where the inclusion of higher energy levels makes a significant difference—PZ's study was based on calculations that included levels with energies up to 71,500 cm^{-1}. This proves to be adequate for their study because, through equation (8), the electron number densities generated by the arc effectively eliminate the need to consider higher energy levels. However, partition functions computed with

this cutoff begin to diverge significantly from values tabulated by Drawin and Felenbok [13] for temperatures above about 15,000 K unless $\Delta E_{i,j}^{\infty}$ exceeds about 4,000 cm^{-1} (0.5 eV). [From equation (4), n_e must exceed about 4×10^{24} m^{-3} at 15,000 K to produce a $\Delta E_{i,j}^{\infty}$ of this magnitude.] A $\Delta E_{i,j}^{\infty}$ of 4,000 cm^{-1} truncates levels with energies greater than 86,900 cm^{-1}, and the partition function calculations for carbon prove to be relatively insensitive to the inclusion or omission of its levels that exist between 71,500 and 86,900 cm^{-1}. [Energy levels with principle quantum numbers equal to 3, 4, and 5 exist in this range.]

In the interest of avoiding database-related limitations beyond those we specifically intended to impose, more wide-ranging agreement with Drawin and Felenbok [13] was sought. (Unfortunately, Drawin and Felenbok do not provide sufficient detail about the bases for their calculations to do them directly.) To get better agreement, energy level data for carbon that included all predicted levels up to $n = 10$ were employed. This information was primarily obtained from references by Moore [14] and Striganov and Sventitskii [15], but also includes predicted levels not found in either of these works. These missing levels were added based on a "fill" procedure that is described in Appendix A. Partition functions computed from Table A-1 (in Appendix A) are in good agreement with those tabulated by Drawin and Felenbok for all $\Delta E_{i,j}^{\infty}$ and temperatures from 2,750 to 20,500 K.

We also note that, as expressed in equations (1)–(8), the concentrations of e^-, C, C^+, C^{++}, H, and H^+ are functions of the temperature and electron number density (T,n_e), not temperature and pressure (T,P) per se. To determine concentrations as a function of temperature and pressure, and thus facilitate direct comparison between the SE model and CEA, we developed an iterative procedure to find the electron number density at a desired temperature and pressure. The first step in the procedure involved setting z equal to 1 (based on the expectation that the concentration of C^{++} would be extremely small) and calculating $\Delta E_{i,j}^{\infty}$ and $Z_{i,j}(T)$ for two values of n_e that bounded the electron density at the desired pressure. For each (n_e, z) pair, species concentrations were derived and an updated estimate for z obtained. The new (n_e, z) pair, in turn, led to a new estimate for the chemical composition (for the given electron number density).

Succeeding estimates were obtained until the chemical composition and z were consistent to nine significant digits.

Once the chemical compositions of the bounding (n_e, z) pairs were established, the pressures corresponding to these pairs were found from the ideal gas law,

$$P = kT\sum_i \left[(\sum_j n_{i,j})(1 + \sum_j j x_{i,j}) \right]. \quad (9)$$

A bisection root-finding technique was then employed to obtain a new estimate for n_e (and chemical composition) whose pressure was closer to the desired value. The convergence criterion for the root finding routine, which is slightly modified version of a program given by Press et al. [16], was set at 1 x 10^{15} m^{-3}. This criterion was selected based on preliminary work that showed that the electron number densities of plasmas considered in this study would be greater than 7 x 10^{19} m^{-3}. Moreover, when this criterion is met, the pressure of the composition is found to agree with the desired pressure to better than six significant digits.

2.2 CEA. The most recent version of CEA of which we are aware (i.e., CEA600) was released in 1998, but we had trouble getting it to run a *"TP"* calculation (i.e., calculate a composition for an assigned temperature and pressure state). Therefore, we reverted to CEA300, which was released in 1997. Like the SE model, CEA employs the ideal gas law to model the equation of state. For the purposes of this study, we modified CEA so that it could be called as a subroutine by a program that handled input and output chores. We also added thermodynamic property data (coefficients) for C^{++} to THERMO.INP. Details of the inclusion of this specie to the data file are described in Appendix B.

2.3 Temperature and Pressure Bounds. The two models are compared for temperatures ranging from 5,000 K to 20,000 K and pressures from 10 bar to 200 bar. The low end of the temperature range was set in recognition of the fact that CEA is well established for temperatures up to 6,000 K. At such temperatures, the concentration of charged particles in a gas composed from C, H, N, and O nuclei will be very small and Coulomb interactions will be negligible. Thus, it is expected that CEA will provide good estimates at such temperatures. The high end of

the temperature range was based on the limit of applicability of the data in THERMO.INP. The pressure range is applicable to ablating-capillary arc dynamics during the ignition phase of the interior ballistics cycle. Higher pressures, which would be pertinent to ETC propulsion concepts in which the plasma is injected later in the interior ballistics cycle, were not considered because the ideal gas equation of state underlying both models becomes a questionable assumption. The calculation of chemical concentrations at high pressures requires the use of a program (such as BLAKE [17]) that is designed to address nonideal behavior. The influence of the equation of state on the chemical composition of an arc is beyond the scope of the present work.

3. Results and Discussion

As developed to date, CEA and the SE model have different inherent limitations: (1) CEA does not have an ability to account for Coulomb interactions, and (2) the SE model has a reaction product data set that is limited to monatomic species. Moreover, they employ different mathematical approaches for establishing equilibrium. Coupled with the fact that CEA is virtually a "black box," these differences have the potential to obscure bases for differences in their results. To address this issue, we first compare results from the models under a set of imposed limitations that highlight "real" differences between them. As points of reference for the comparisons to be shown, model computations for the temperature dependence of plasma compositions at a pressure of 50 bar are shown in Figures 1 and 2.

As a first comparison of the two approaches, the reaction product set employed in CEA is limited to those species (e^-, C, C^+, C^{++}, H, and H^+) considered in the SE model, and the ionization potential reduction parameter ($\Delta E_{i,j}^{\infty}$) of the SE model is set equal to 0. Modified in this manner, the two approaches (should, in principle,) become mathematically equivalent. As such, it was expected that the models would yield the same results. As shown in Figure 3, this expectation is (essentially) realized for all species except C^{++} for temperatures from 5,000 to 15,000 K, the difference in predicted species concentrations being less than 5% over this temperature range. (In view of the fact that C^{++} concentrations are more than 3 orders of magnitude less than any

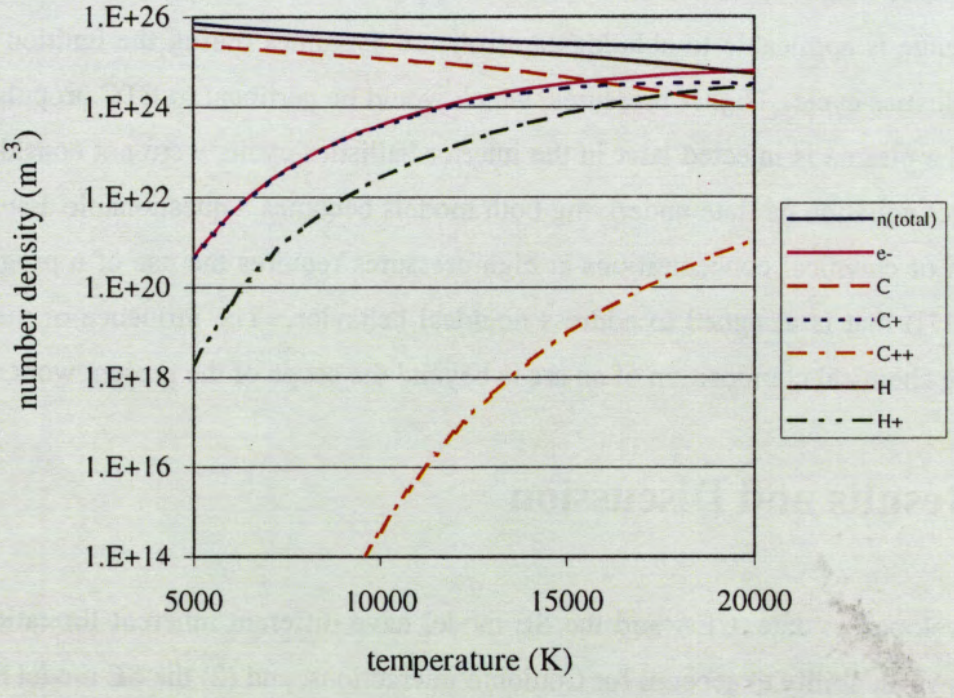

Figure 1. SE Model Calculations of Reaction Product Number Densities vs. Temperature for a 50-bar Gas Formed From Decomposed Polyethylene.

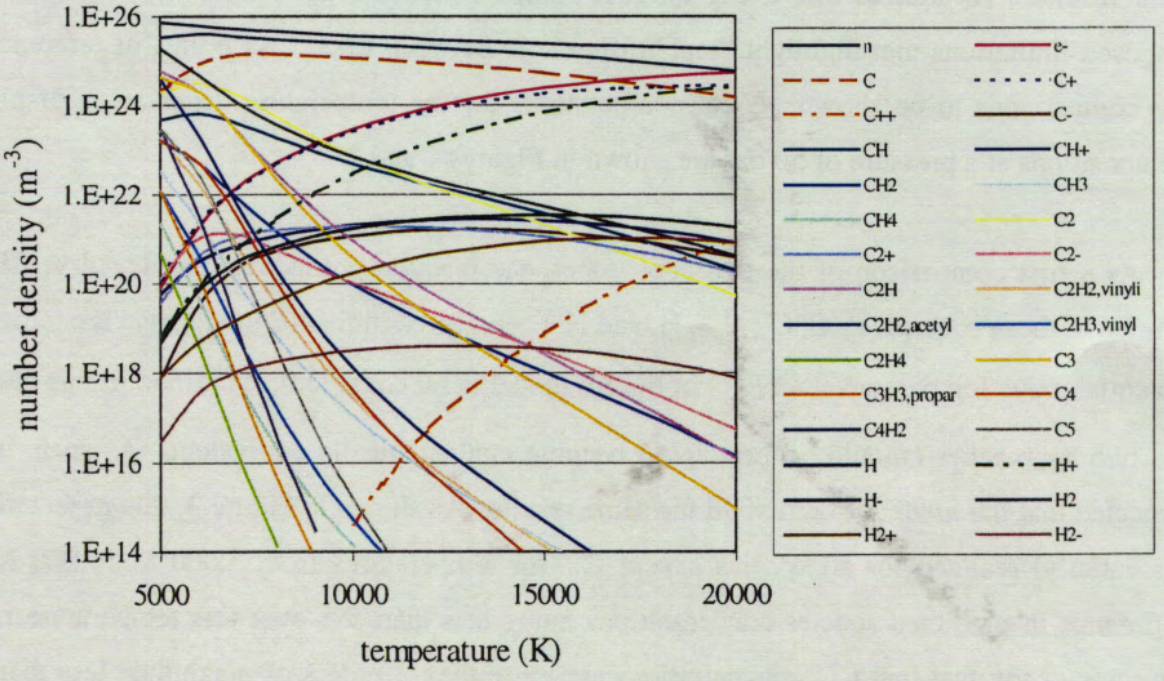

Figure 2. CEA Calculations of Reaction Product Number Densities vs. Temperature for a 50-bar Gas Formed From Decomposed Polyethylene.

other specie, the results for C^{++} can be discounted.) However, as the temperature increases above this range, the predictions of the two models begin to diverge significantly.

We suspected that the differences observed as the temperature increases above 15,000 K are due to differences in the number of energy levels employed to compute the thermodynamic property data of carbon given in THERMO.INP and those employed to compute carbon's partition function for the SE model. This suspicion is borne out by the results shown in Figure 4, which compares (1) carbon's heat capacity as computed by the THERMO.INP coefficients, and (2) the approach outlined in Appendix B, where energy levels with principle quantum numbers up to $n = 10$ have been used for the computation. To verify that the difference is due to fewer energy levels being employed in the procedure to generate the coefficients in THERMO.INP, heat capacity values calculated when energy levels above 71,500 cm^{-1} are excluded are shown for comparison. This result suggests that the "TEMPER method" [18] has been employed to derive the THERMO.INP coefficients for carbon atoms. (In this method, $E_{i,j}^{\infty}$ is lowered as a function of the temperature.) If the limited energy level set employed to generate Figure 4 (c) is employed for SE model calculations of chemical composition, the results obtained from the two models are in good agreement for the entire temperature range considered (see Figure 5). (Again, the relatively large differences observed for C^{++} are related to the fact that it is present in trace amounts.)

The results shown in Figure 5 suggest the equivalence of truncating the partition function summation in the SE model [per equation (8)] and restricting the number of levels used for the calculation of thermodynamic properties. The cutoff expressed in the thermodynamic property data does not, however, lower C^{+} (or C^{++}) energy levels relative to C. That is, CEA does not have a counterpart to the influence of $\Delta E_{i,j}^{\infty}$ in the SE model as realized through its inclusion in the exponential term of equation (1). This limits the correspondence that can be achieved between the two approaches by simply limiting the energy levels considered in the generation of the thermodynamics data contained in THERMO.INP. This lack of correspondence is observable in the results presented in Figure 6, which compares results obtained when the reaction product set employed by CEA is limited to those species considered in the SE model

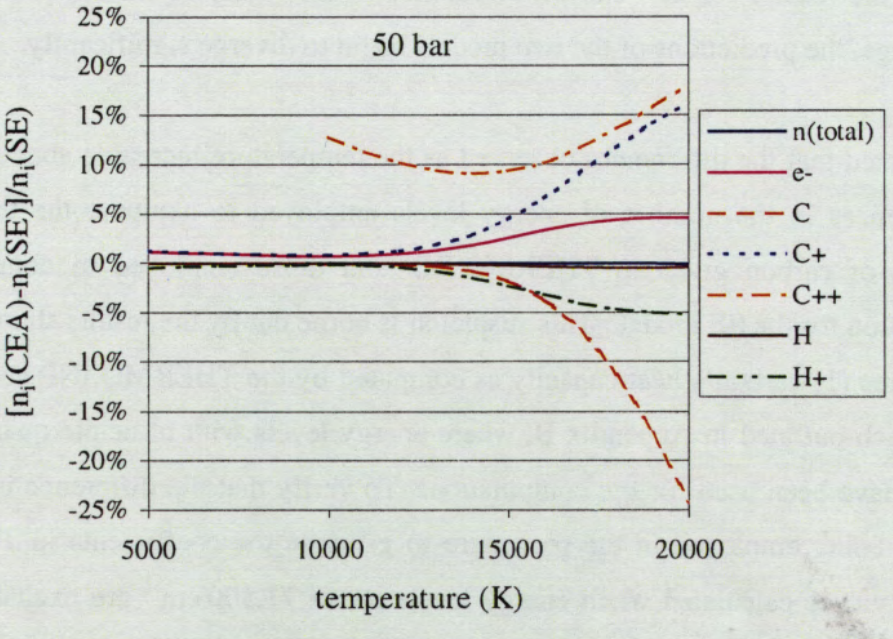

Figure 3. $[n_i(\text{CEA}) - n_i(\text{SE})]/n_i(\text{SE})$ When CEA Employs a Limited Reaction Product Set (e^-, C, C^+, C^{++}, H, and H^+) and the SE Model Has $\Delta E^{\circ}_{i,j} = 0$.

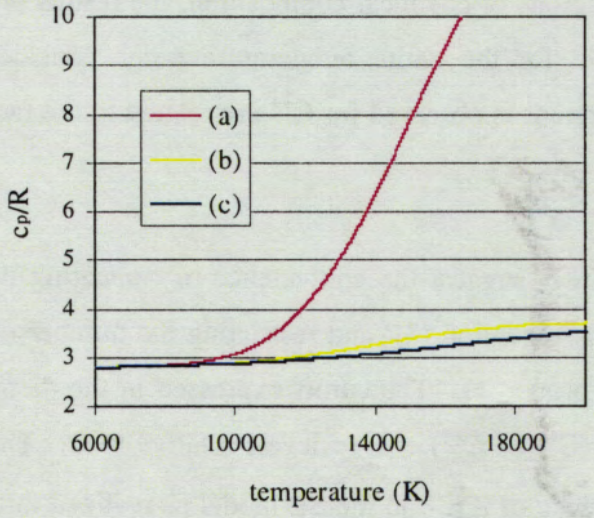

Figure 4. The Dimensionless Heat Capacity of Neutral Carbon Atoms as Computed by (a) the Method Outlined in Appendix B With Energy Levels up to 89,800 cm^{-1} Included, (b) the Coefficients in THERMO.INP, and (c) the Method Outlined in Appendix B With Energy Levels up to 71,500 cm^{-1} Included.

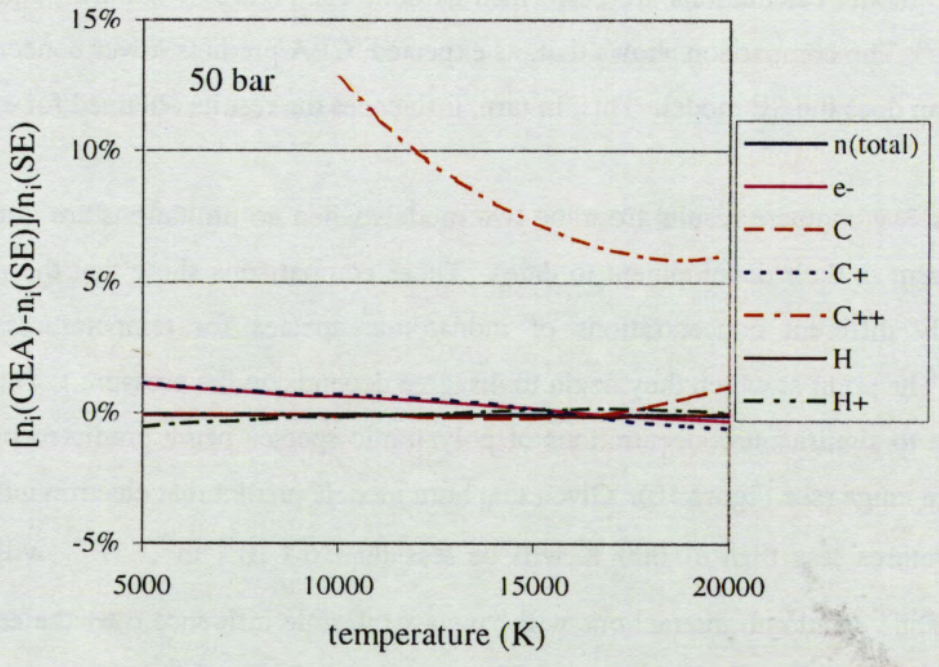

Figure 5. $[n_i(\text{CEA}) - n_i(\text{SE})]/n_i(\text{SE})$ When CEA Employs a Limited Reaction Product Set and the SE Model Employs $\Delta E^{\infty}_{i,j} = 0$, $E^k \leq 71{,}500$ cm^{-1} for Partition Function Calculations.

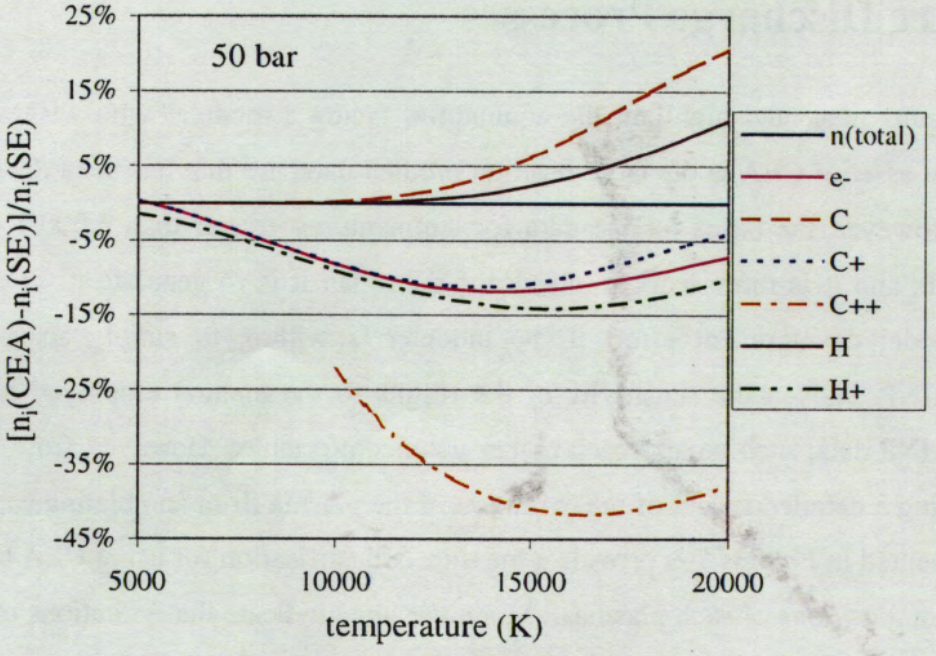

Figure 6. $[n_i(\text{CEA}) - n_i(\text{SE})]/n_i(\text{SE})$ When CEA Employs a Limited Reaction Product Set and the SE Model Employs $E^k \leq 71{,}500$ cm^{-1} for Partition Function Calculations.

and the SE model calculations are performed as done for Figure 5, but with equation (4) now "turned on." The comparison shows that, as expected, CEA predicts lower concentrations of C^+ and C^{++} than does the SE model. This, in turn, influences the results obtained for e-, H, and H^+.

Figures 7–9 compare results from the two models when no limitations are imposed (beyond those inherent in their development to date). These comparisons show that the models predict significantly different concentrations of monatomic species for temperatures below about 8,000 K. (The point at which they begin to disagree depends on the pressure.) This difference is attributable to significant concentrations of polyatomic species being predicted by CEA in this temperature range (see Figure 10). Given that both models predict that electron number densities for temperatures less than 10,000 K will be less than 6×10^{23} m^{-3}, $\Delta E_{i,j}^{\infty}$ will be less than 0.15 eV. Thus, Coulomb interactions will have a negligible influence over the equilibrium. In view of these considerations, we expect CEA to provide estimates that are superior to those from the SE model in the temperature range below 8,000 K.

4. Considerations Related to Modeling Ablating-Capillary Arc Discharge Processes

The results presented highlight the conundrum facing a modeler who wishes to use CEA. The biggest asset of CEA is the large reaction product database that has been developed for use with it. However, the bases for the data for temperatures greater than 6,000 K are relatively inaccessible, and it is more work to check the data than it is to generate it. Thus, CEA only reduces model development effort if the modeler is willing to simply accept the data in THERMO.INP. Given the sensitivity of the results to the method employed to generate the THERMO.INP data, such an approach makes us uncomfortable. However, from the standpoint of developing a detailed model of the evolution of the plasma from an ablating capillary arc, the results presented in Figures 7–9 provide a measure of justification for using CEA to calculate the chemical compositions of such plasmas. Moreover, they indicate the limitations of an SE model that utilizes a reaction product database that includes only monatomic species.

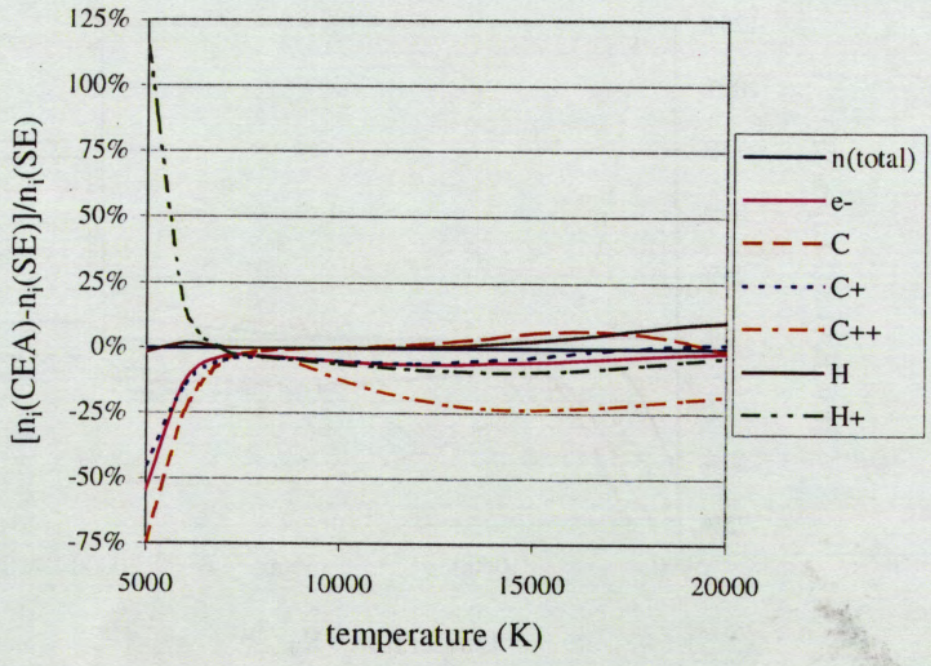

Figure 7. $[n_i(\text{CEA}) - n_i(\text{SE})]/n_i(\text{SE})$ at a Pressure of 10 bar.

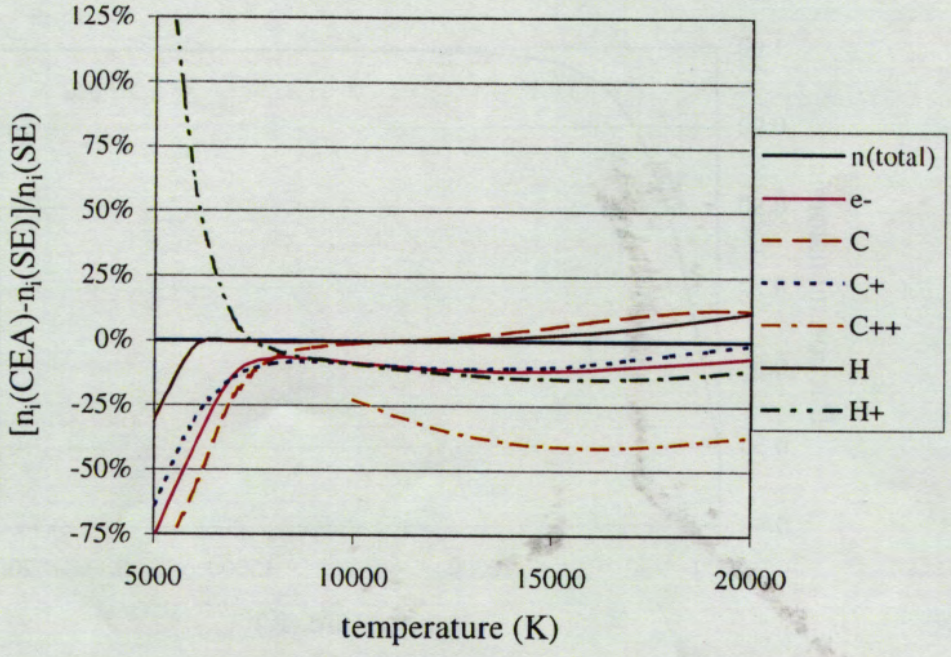

Figure 8. $[n_i(\text{CEA}) - n_i(\text{SE})]/n_i(\text{SE})$ at a Pressure of 50 bar.

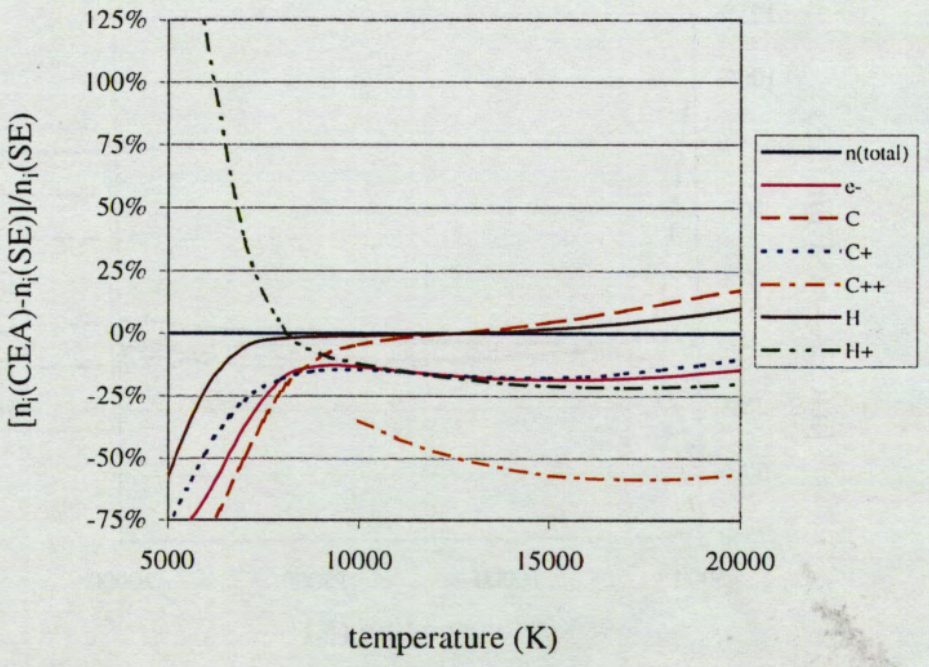

Figure 9. $[n_i(\text{CEA})-n_i(\text{SE})]/n_i(\text{SE})$ at a Pressure of 200 bar.

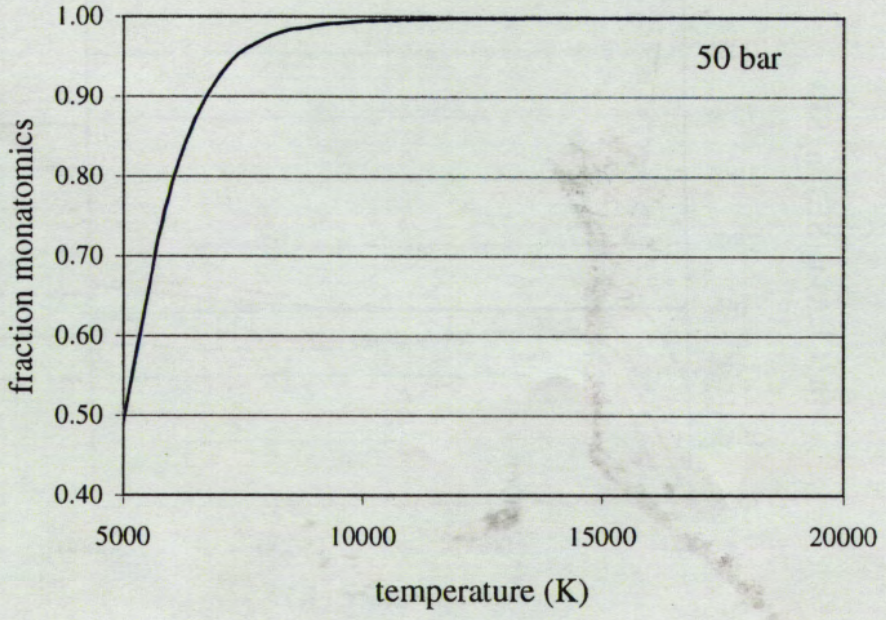

Figure 10. CEA Calculation of the Fraction of Total Heavy Nuclei-Containing Particles That Are Monatomic.

As an initial step toward developing a CFD model of ablating-capillary arc ignition, we are using the PZ model of arc dynamics to calculate the temperature and pressure (state) of the effluent at the capillary exit plane and using CEA to calculate the composition for this state. The PZ model calculations of constituent densities are disregarded. Of course, the dynamics of the ablating capillary arc process depend on the constituent densities in the arc, and thus this approach is internally inconsistent. An aspect of this inconsistency is shown in Figure 11, which compares the effective molecular weight of the plasma at the same temperature and pressure as computed by CEA and the SE model. However, this inconsistency is considered tolerable when judged from the standpoint of developing a detailed model of the discharge process. By its nature, such a development effort needs to be done incrementally, and CEA has allowed us to make timely preliminary assessments of the impact of polyatomic species on the evolution of the plasma outside the capillary [6]. The results obtained with this approach are also providing guidance for efforts to build the reaction mechanisms and transport coefficient data needed for the CFD model [6, 19]. And such benefits will have even greater importance when systems with N- and O-containing species are considered, their chemical compositions being much more complex than the "hydrocarbon" plasmas considered here.

In the course of this study, an approach for incorporating the effect of Coulomb interactions into a Gibb's free-energy minimization calculation of chemical compositions was identified [20, 21], and we consider that CEA could be modified to incorporate this approach. However, the data in THERMO.INP would probably also need to be modified, effectively voiding the potential benefit of such an undertaking. Moreover, CEA is relatively inconvenient to use as a subroutine, and trying to modify the PZ code to utilize it (and thus resolving the inconsistency) is not an attractive option. Therefore, as the next step in code development, we intend to develop a new model of ablating capillary arc dynamics that is integral to the CFD model and to write our own subroutine for chemical composition calculations. (The mathematical approach we will employ remains to be decided.) This effort will resolve the inconsistency inherent in the current approach [6], and it will facilitate our ability to model the coupling between arc dynamics and processes occurring outside the capillary.

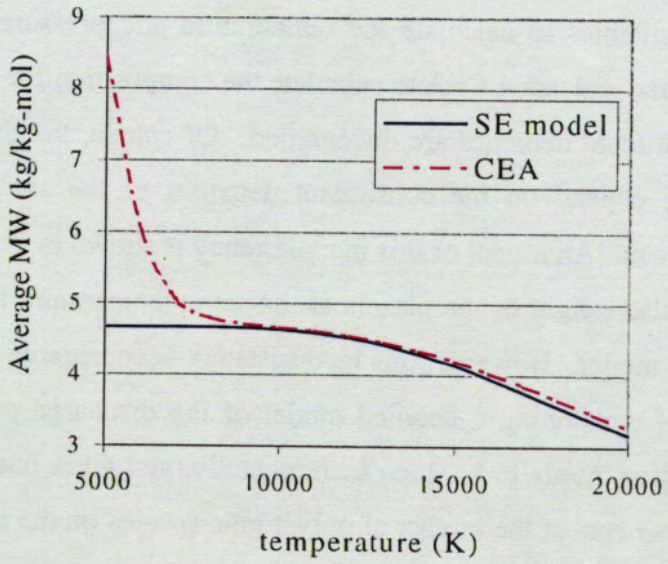

Figure 11. The Average Molecular Weight of 50-bar Plasmas as Computed by CEA and the SE Model.

5. Conclusions

The chemical compositions of plasmas created from decomposed polyethylene as computed by (1) the NASA-Lewis computer program for the calculation of complex chemical equilibrium (CEA) and (2) an SE model with a limited reaction product set have been compared. Results are presented for temperatures from 5,000 to 20,000 K and pressures from 10 to 200 bar, conditions that are relevant to modeling an ablating-capillary arc discharge during the ignition phase of an interior ballistic cycle. The study was undertaken to establish whether CEA could be used to generate source species concentrations for a CFD model being developed to characterize plasma-propellant interactions. The results indicate that even though CEA does not account for Coulomb interactions, its estimates of chemical composition should be adequate for this application.

6. References

1. Katulka, G. L., and J. Dyvik. "Experimental Results of Electrical Plasma Ignition in 120-mm Solid Propellant Tank Gun Firings." *Proceedings of the 33rd JANNAF Combustion Subcommittee Meeting*, CPIA Publication 653, vol. 3, pp. 103–110, 1996.

2. Powell, J. D., and A. E. Zielinski. "Theory and Experiment for an Ablating-Capillary Discharge and Application to Electrothermal-Chemical Guns." BRL-TR-3355, U.S. Army Ballistic Research Laboratory, Aberdeen Proving Ground, MD, 1992.

3. Del Guercio, M. "Propellant Burn Rate Modification by Plasma Injection." *Proceedings of the 34th JANNAF Combustion Subcommittee Meeting*, CPIA Publication 662, vol. 1, pp. 35–42, 1997.

4. Perelmutter, L., M. Sudai, C. Goldenberg, D. Kimhe, Z. Zeevi, S. Arie, M. Melnik, and D. Melnik. "Temperature Compensation by Controlled Ignition Power in SPETC Guns." *Proceedings of the 16th International Symposium on Ballistics*, pp. 145–152, 1996.

5. Dyvik, J., and G. Katulka. "ETC Temperature Compensation: Experimental Results of 120-mm Test Firings." CPIA Publication 653, vol. 3, pp. 111–119, 1995.

6. Nusca, M. J., and M. J. McQuaid. "Modeling the Open-Air Plasma Jet from and ETC Igniter Using a Multi-Species Reacting Flow CFD Code." *Proceedings of the 36th JANNAF Combustion Subcommittee Meeting*, to be published.

7. Nusca, M. J., K. J. White, A. W. Williams, A. M. Landsberg, T. R. Young, and C. A Lind. "Computational and Experimental Investigations of Open-Air Plasmas Discharges." *Proceedings of the 37th AIAA Aerospace Sciences Meeting*, AIAA Paper No. 99-0865, 1999.

8. Griem, H. R. *Plasma Spectroscopy*. New York: McGraw-Hill Book Co., 1964.

9. Kappen, K., and U. H. Bauder. "Simulation of Plasma Radiation in Electrothermal Chemical Accelerators," *IEEE Transactions in Magnetics*, vol. 35, pp. 192–200, 1999.

10. McBride, B. J., and S. Gordon. "Computer Program for Calculation of Complex Chemical Equilibrium Compositions and Applications II. User's Manual and Program Description." NASA Reference Publication 1311, NASA Lewis Research Center, Cleveland, OH, 1996.

11. Gordon, S., and B. J. McBride. "Computer Program for Calculation of Complex Chemical Equilibrium Compositions and Applications I. Analysis." NASA Reference Publication 1311, NASA Lewis Research Center, Cleveland, OH, 1994.

12. Eberling, W., and R. Sandig. "Theory of the Ionization Equilibrium in Dense Plasmas." *Annullen der Physik*, vol. 28, p. 289, 1973.

13. Drawin, H.-W., and P. Felenbok. *Data for Plasmas in Local Thermodynamic Equilibrium.* Paris: Gauthier-Villars, 1965.

14. Moore, C. E. "Atomic Energy Levels as Derived from the Analyses of Optical Spectra. Vol I, ^{1}H to ^{23}V." NBS-NSRDS 35, National Bureau of Standards, Washington, DC, 1948.

15. Stiganov, A. R., and N. S. Sventitskii. *Tables of Spectral Lines of Neutral and Ionized Atoms*. New York: IFI/Plenum, 1968.

16. Press, W. H., B. P. Flannery, S. A. Teukolsky, and W. T. Vetterling. *Numerical Recipes: The Art of Scientific Computing (Fortran Version).* Cambridge: Cambridge University Press, 1989.

17. Oberle, W., and E. Freedman. "Preparation and Extension of the Thermodynamics Program BLAKE and Its Library to 10,000 K for Use with Electrothermal-Chemical Systems." ARL-TR-488, U.S. Army Research Laboratory, Aberdeen Proving Ground, MD, 1994.

18. McBride, B. J., and S. Gordon. "Computer Program for Calculating and Fitting Thermodynamic Functions." NASA Reference Publication 1271, NASA Lewis Research Center, Cleveland, OH, 1992.

19. Anderson, W. R., and M. A. Schroeder. "Chemical Mechanism for ETC Plasma Interaction with Air." *Proceedings of the 36th JANNAF Combustion Subcommittee Meeting*, to be published.

20. Kovitya, P. "Physical Properties of High-Pressure Plasmas of Hydrogen and Copper in the Temperature Range 5,000-60,000 K." *IEEE Transactions on Plasma Science*, vol. PS-13, pp. 587–594, 1985.

21. Kappen, K. *Berechnung der Materialfunktionen von Hochdruckplasmen am Beispiel von Methanol.* Diplomarbeit, Technishe Universtat Munchen, 1994.

Appendix A:

Fill and Cutoff Procedures Used to Establish the Energy Level Structure for Carbon

INTENTIONALLY LEFT BLANK.

The calculation of the electronic partition function,

$$Z_{i,j}(T) = \sum_k g_{i,j,k} \exp\left(\frac{-E_{i,j}^k}{k_b T}\right), \tag{A1}$$

for plasma specie (i,j) at a temperature (T) requires knowledge of its energy levels $(E_{i,j}^k)$, their statistical weights $(g_{i,j,k.})$, and a procedure to address the fact that the sum is not intrinsically bound. In a plasma, the latter concern is typically resolved by truncating the summation at a level, *max*, set by

$$E_{i,j}^{\max} \le E_{i,j}^{\infty} - \Delta E_{i,j}^{\infty}, \tag{A2}$$

where $E_{i,j}^{\infty}$ is the ionization potential of the specie and $\Delta E_{i,j}^{\infty}$ is the reduction in the ionization potential resulting from its interaction with charged particles. This is referred to as a cutoff procedure and will depend on one's choice of ionization potential reduction theory.

Energy level information for atomic species can be found in a number of references, with Moore's tables[1] being perhaps the most widely used. However, usually only levels with low values of orbital angular momentum are known, and such tables are almost always incomplete below the limit given by equation (A2). In the case of (neutral) carbon, Moore's table does not include any information on f or higher levels of orbital angular momentum, and information on any n level becomes sparser as n increases. This turns out to be a significant issue for temperatures above about 15,000 K. The issue arises because carbon has a relatively low ionization potential—$I_{C,1}$ = 90,878 cm^{-1} (11.3 eV) vs. $I_{H,1}$ = 109,679 cm^{-1} (13.6 eV), $I_{N,1}$ = 117,345 cm^{-1} (14.5 eV), and $I_{O,1}$ = 109,837 cm^{-1} (13.6 eV)—and high principle quantum numbers (with statistical weights proportional to n^2) are present at relatively low energies.[1] (For example, n = 4 levels of carbon are observed between 9.7 and 10.5 eV, while in hydrogen, these

[1]Moore, E. "Atomic Energy Levels as Derived from the Analyses of Optical Spectra. Vol I, ^{1}H to ^{23}V," NBS-NSRDS 35, National Bureau of Standards, Washington, DC, 1948.

levels are observed at 12.7 eV.) Since these "missing" levels have high statistical weights, their omission can lead to serious errors.

For temperatures above about 15,000 K, we found that if partition functions were computed based on using the energy levels listed by Moore alone, they were significantly lower than those tabulated by Drawin and Felenbok[2] unless $\Delta E_{i,j}^{\infty}$ was greater than about 4,000 cm^{-1} (0.5 eV). As a first step toward completing (or "filling") Moore's table for carbon, we relied on the spectroscopic data tabulated by Striganov and Sventitskii[3] to identify "missing" levels. Their assignments of the data in their tables provided the 4f levels (84,050 cm^{-1}) and a number of n = 5, 6, 7, and 8 levels. For remaining levels (up to n = 10), we estimated energy level values based on trends in the observed levels. For example, we specified the energy level of the 5g levels to be 86,570 cm^{-1} based on our expectation that these levels would be higher in energy than the 5f levels (86,470 cm^{-1}), but by a value less than the separation between 5f and 5d levels (170 cm^{-1}).

Table A-1 shows the data used for computing partition functions in this study. (In order to reduce the size of the table, spin-multiplet terms from Moore's table are combined and term values limited to three significant digits, but five significant digits were used in the actual computations.) All predicted levels with energies up to 89,800 cm^{-1} are included. The partition functions generated with this table were found to be less than 3% different from those tabulated by Drawin and Felenbok[2] for all $\Delta E_{i,j}^{\infty}$ and temperatures from 2,750 K to 20,500 K. The highest energy level included in the table (89,800 cm^{-1}) corresponds to an implicit $\Delta E_{i,j}^{\infty}$ minimum of 1,100 cm^{-1} (0.15 eV). If n = 11 levels are included—11d ^{3}D being observed at 89,968 cm^{-1}—they begin to make a significant contributions to the partition function as the temperature approaches 20,000 K. But we expect that such levels will not "exist" for plasmas at the densities generated by an ablating-capillary arc.

---

[2]Drawin, H.-W., and P. Felenbok. *Data for Plasmas in Local Thermodynamic Equilibrium.* Paris: Gauthier-Villars, 1965.

[3]Stiganov, A. R., and N. S. Sventitskii. *Tables of Spectral Lines of Neutral and Ionized Atoms.* New York: IFI/Plenum, 1968.

In the cases of C^+ and C^{++}, the levels listed in Moore's table proved sufficient for the temperature range of interest. The levels employed for the calculations of these species are shown in Tables A-2 and A-3. The decision on the highest level to include for this study was based, in part, on considering that only levels to 89,800 cm^{-1} were retained for carbon. Comparison with Drawin and Felenbok's[2] data provide a basis for the adequacy of these data sets for temperatures to 20,000 K.

In the case of hydrogen, we calculated its energy levels (in wavenumbers) and their statistical weight using

$$E_{H,1}^{k} = 109{,}679\left(1 - \frac{1}{k^2}\right)$$

and

$$g_{H,1,k} = 2k^2,$$

respectively. Levels up to $k = 4$ were allowed. Again, comparison with the partition functions tabulated by Drawin and Felenbok[2] provided a basis for the adequacy of this approach for temperatures from 5,000 to 20,000 K.

---

[2]Drawin, H.-W., and P. Felenbok. *Data for Plasmas in Local Thermodynamic Equilibrium.* Paris: Gauthier-Villars, 1965.

Table A-1. Energy Levels and Statistical Weights Employed to Compute Partition Functions for Carbon

Design	g	Level (cm^{-1})	Source	Design	g	Level (cm^{-1})	Source
$2p^2\ ^3P$	1	0.0	Moore 1948	$5p\ ^1D$	5	85,400	Moore 1948
	3	16.4	Moore 1948	$5p\ ^1S$	1	85,626	Moore 1948
	5	43.5	Moore 1948	$5d\ ^1D$	5	86,187	Moore 1948
$2p^2\ ^1D$	5	10,194	Moore 1948	$5d\ ^3F$	5,7,9	86,300	Moore 1948
$2p^2\ ^1S$	1	21,648	Moore 1948	$6s\ ^3P$	9	86,310	Stiganov 1968
$2p^3\ ^5S$	3	33,735	Moore 1948	$5d\ ^3D$	3,5,7	86,400	Moore 1948
$3s\ ^3P$	1,3,5	60,300	Moore 1948	$6s\ ^1P$	3	86,400	Moore 1948
$3s\ ^1P$	3	61,982	Moore 1948	$5d\ ^1F$	7	86,400	Moore 1948
$2p^3\ ^3D$	7,5,3	64,100	Moore 1948	5f *	84	86,470	Stiganov 1968
$3p\ ^1P$	3	68858	Moore 1948	$5d\ ^1P$	3	86,500	Moore 1948
$3p\ ^3D$	3,5,7	69,700	Moore 1948	$5d\ ^3P$	5,3,1	86,500	Moore 1948
$3p\ ^3S$	3	70,744	Moore 1948	5g *	108	86,650	Author Estimate
$3p\ ^3P$	1,3,5	71,400	Moore 1948	6p *	36	87,000	Author Estimate
$3p\ ^1D$	5	72,611	Moore 1948	$6d\ ^1D$	5	87,632	Moore 1948
$3p\ ^1S$	1	73,976	Moore 1948	$6d\ ^3F$	5,7,9	87,700	Moore 1948
$2p^3\ ^3P$	5,3,1	75,300	Moore 1948	$6d\ ^3D$	3,5,7	87,800	Moore 1948
$3d\ ^1D$	5	77,680	Moore 1948	$7s\ ^1P$	3	87,795	Moore 1948
$4s\ ^3P$	1,3,5	78,100	Moore 1948	6f *	84	87,800	Stiganov 1968
$3d\ ^3F$	5,7,9	78,200	Moore 1948	$7s\ ^3P$	9	87,800	Stiganov 1968
$3d\ ^3D$	3,5,7	78,300	Moore 1948	$6d\ ^1F$	7	87,807	Moore 1948
$4s\ ^1P$	3	78,338	Moore 1948	$6d\ ^3P$	5,3,1	87,800	Moore 1948
$3d\ ^1F$	7	78,531	Moore 1948	$6d\ ^1P$	3	87,831	Moore 1948
$3d\ ^1P$	3	78,728	Moore 1948	6g *	108	87,850	Author Estimate
$3d\ ^3P$	5,3,1	79,300	Moore 1948	6h *	132	87,900	Author Estimate
$4p\ ^3D$	3,5,7	80,200	Moore 1948	7p *	36	88,200	Author Estimate
$4p\ ^1P$	3	80,564	Moore 1948	$7d\ ^3F$	5,7,9	88,500	Moore 1948
$4p\ ^3S$	3	81,106	Moore 1948	$7d\ ^3D$	3,5,7	88,607	Moore 1948
$4p\ ^3P$	1,3,5	81,300	Moore 1948	$7d\ ^1F$	7	88,624	Moore 1948
$4p\ ^1D$	5	81,770	Moore 1948	$7d\ ^1P$	3	88,632	Moore 1948
$4p\ ^1S$	1	82,252	Moore 1948	$7d\ ^3P$	5,3,1	88,639	Moore 1948
$4d\ ^1D$	5	83,500	Moore 1948	8s *	12	88,560	Stiganov 1968
$5s\ ^3P$	9	83,730	Stiganov 1968	$7d\ ^1D$	5	88,600	Author Estimate
$4d\ ^3F$	5	83,761	Moore 1948	8p *	36	88,850	Author Estimate
$4d\ ^3D$	3,5,7	83,800	Moore 1948	7f-i *	480	89,000	Author Estimate
$5s\ ^1P$	3	83,882	Moore 1948	8d-j *	720	89,100	Moore 1948, Author Estimate
$4d\ ^1F$	7	83,949	Moore 1948	9s *	12	89,100	Author Estimate
$4d\ ^1P$	3	84,032	Moore 1948	9P *	36	89,300	Moore 1948
4f *	84	84,050	Stiganov 1968	9d-k *	924	89,500	Moore 1948, Author Estimate
$4d\ ^3P$	5,3,1	84,100	Moore 1948	10s *	12	89,500	Author Estimate
$5p\ ^1P$	3	84,852	Moore 1948	10p *	36	89,650	Author Estimate
$5p\ ^3D$	3,5,7	85,000	Moore 1948	10d-1 *	1152	89,800	Moore 1948, Author Estimate
$5p\ ^3S/^3P$	12	85,000	Author Estimate				

Table A-2. C^+ Term Values Used for Partition Function Computations[a]

Designation	g	Level (cm^{-1})
$2p\ ^2P$	2	0.0
	4	64.0
$2p\ ^4P$	2	43,000
	4	43,022
	6	43,051
$2p\ ^2D$	6	74,931
	4	74,933
$2p\ ^2S$	2	96,494

[a]Moore, C. E. "Atomic Energy Levels as Derived from the Analyses of Optical Spectra. Vol. I, ^1H to ^{23}V." NBS-NSRDS 35, National Bureau of Standards, Washington, DC, 1948.

Table A-3. C^{++} Term Values Used for Partition Function Computations[a]

Designation	g	Level (cm^{-1})
$2s^2\ ^1S$	1	0.0
$2p\ ^3P$	1	52,315
	3	52,338
	5	52,395
$2p\ ^1P$	1	102,351

[a]Moore, C. E. "Atomic Energy Levels as Derived from the Analyses of Optical Spectra. Vol. I, ^1H to ^{23}V." NBS-NSRDS 35, National Bureau of Standards, Washington, DC, 1948.

INTENTIONALLY LEFT BLANK.

Appendix B:

Thermodynamic Properties for C^{++}

INTENTIONALLY LEFT BLANK.

The NASA-Lewis computer program for the calculation of complex chemical equilibrium compositions[1] (CEA) establishes the equilibrium state of a system by minimizing the Gibb's free energy of a reaction product set. To calculate the Gibb's free energy for the set, it relies on a library of thermodynamic property data (THERMO.INP) for computing the heat capacity [$C_p(T)$], enthalpy [$H^o(T)$], and entropy [$S^o(T)$] of each product at a temperature (T). The library consists of a set of product-specific coefficients (a_i, b_i) that yield these properties via the empirical equations,

$$\frac{C_p^o(T)}{R} = a_1 T^{-2} + a_2 T^{-1} + a_3 + a_4 T + a_5 T^2 + a_6 T^3 + a_7 T^4, \tag{B1}$$

$$\frac{H^o(T)}{RT} = -a_1 T^{-2} + a_2 T^{-1} \ln T + a_3 + a_4 \frac{T}{2} + a_5 \frac{T^2}{3} + a_6 \frac{T^3}{4} + a_7 \frac{T^4}{5} + \frac{b_1}{T}, \tag{B2}$$

and

$$\frac{S^o(T)}{R} = -a_1 \frac{T^{-2}}{2} + a_2 T^{-1} + a_3 \ln T + a_4 T + a_5 \frac{T^2}{2} + a_6 \frac{T^3}{3} + a_7 \frac{T^4}{4} + b_2, \tag{B3}$$

where R is the universal gas constant. This appendix describes the determination of such coefficients for C^{++}. Though concentrations of C^{++} in any system at temperatures ≤ 20,000 K are likely to be very small, this exercise was undertaken in the interest of conducting as complete a comparison as possible between CEA and the SE model employed by Powell and Zielinski.[2]

---

[1]McBride, B. J., and S. Gordon. "Computer Program for Calculation of Complex Chemical Equilibrium Compositions and Applications II. User's Manual and Program Description." NASA Reference Publication 1311, NASA Lewis Research Center, Cleveland, OH, 1996.

[2]Powell, J. D., and A. E. Zielinski. "Theory and Experiment for an Ablating-Capillary Discharge and Application to Electrothermal-Chemical Guns." BRL-TR-3355, U.S. Army Ballistic Research Laboratory, Aberdeen Proving Ground, MD, 1992.

As a first step toward determining the (a_i, b_i) coefficients for C^{++}, $C_p(T)$, $H^o(T)$, and $S^o(T)$ were calculated for temperatures from 298.15 to 20,000 K using the standard definitions,[3]

$$\frac{C_p^o(T)}{R} = \frac{5}{2} + T^2 \frac{d^2 \ln Z(T)}{dT^2} + 2T \frac{d \ln Z(T)}{dT}, \tag{B5}$$

$$\frac{H^o(T)}{RT} = \frac{5}{2} + T \frac{dlnZ(T)}{dT} + \frac{H^o(0\,K)}{RT}, \tag{B6}$$

and

$$\frac{S^o(T)}{R} = \frac{5}{2} + \ln\left(\frac{k_b T}{p^o}\left(\frac{2\pi k_b T}{N_a h^2}\right)^{3/2}\right) + T \frac{d \ln Z(T)}{dT} + \ln Z(T), \tag{B7}$$

where N_a is Avogadro's number and p^o is standard pressure. The enthalpy of formation for C^{++} at 0 K [$H^o(0\,K)$ = 4,150 kJ/mole] was determined from the heat of formation of C^+ given in the NIST/JANAF thermochemical tables[3] and the ionization potential of C^+ given by Moore.[4] Following from the definition of the partition function, the terms with derivatives were computed per

$$T \frac{d \ln Z(T)}{dT} = \frac{1}{k_b T Z(T)} \sum_k g_k E^k \exp\left(\frac{-E^k}{k_b T}\right) \tag{B8}$$

and

[3]Chase, M. W. (ed.) *NIST-JANAF Thermochemical Tables.* 4th edition, *Journal of Physical and Chemical Reference Data*, Monograph No. 9, New York: American Institute of Physics, 1998.

[4]Moore, C. E. "Atomic Energy Levels as Derived from the Analyses of Optical Spectra. Vol I, ^1H to ^{23}V." NBS-NSRDS 35, National Bureau of Standards, Washington, DC, 1948.

$$T^2 \frac{d^2 \ln Z(T)}{dT^2} = \frac{1}{k_b T Z(T)} \left[\sum_k \left(\frac{E^k}{k_b T} - 2 - \frac{1}{k_b T Z(T)} \sum_k g_k E^k \exp\left(\frac{-E^k}{k_b T} \right) \right) g_k E^k \exp\left(\frac{-E^k}{k_b T} \right) \right]. \quad \text{(B9)}$$

The energy level information (E^k and g_k) needed for these computations were extracted from Moore's tables.[4] Table B-1 shows the energy levels employed for the computations. Partition functions computed with these data compare favorably with those tabulated by Drawin and Felenbok.[5] The program to compute thermodynamic properties was checked by running it with the data listed in Appendix A for carbon and verifying that the thermodynamic property data for carbon tabulated in NIST/JANAF thermochemical tables[3] were reproduced.

To determine the a_i coefficients, a nonlinear least squares fitting routine was employed to fit equation (B1) to the plot of $C_p(T)/R$ vs. T computed via equation (B4). The a_i coefficients determined in this manner were then used in fits of (B2) and (B3) to $H^o(T)/RT$ vs. T and $S^o(T)/R$ vs. T, respectively—the fits yielding b_1 and b_2, respectively. Consistent with the practice in the data file, coefficient sets were separately determined for the temperature ranges 298.15–1,000 K, 1,000–6,000 K, and 6,000–20,000 K. The coefficients we inserted into THERMO.INP for this study are given in Table B-2. We note, however, that this table is primarily for informational purposes. Gordon and McBride use routines that simultaneously (rather than sequentially) fit the thermodynamic property functions. Furthermore, the fits are constrained so that the polynomials coefficients employed on either side of a transition point (1,000 and 6,000 K) yield the same value at the transition point. The coefficients are also determined such that, within certain limits, the polynomials may be extrapolated to beyond the range for which they were established. We did not attempt to include such considerations.

---

[3]Chase, M. W. (ed.) *NIST-JANAF Thermochemical Tables*. 4th edition, *Journal of Physical and Chemical Reference Data*, Monograph No. 9, New York: American Institute of Physics, 1998.

[4]Moore, C. E. "Atomic Energy Levels as Derived from the Analyses of Optical Spectra. Vol I, ^{1}H to ^{23}V." NBS-NSRDS 35, National Bureau of Standards, Washington, DC, 1948.

[5]Drawin, H.-W., and P. Felenbok. *Data for Plasmas in Local Thermodynamic Equilibrium*. Paris: Gauthier-Villars, 1965.

Table B-1. C^{++} Term Values and Statistical Weights Used in Computation of Thermodynamic Property Data[a]

Designation	g	Level (cm^{-1})
$2s^2\ ^1S$	1	0.0
$2p\ ^3P$	1	52315
	3	52338
	5	52395
$2p\ ^1P$	3	102351

[a]Moore, C. E. "Atomic Energy Levels as Derived from the Analyses of Optical Spectra. Vol. I, ^1H to ^{23}V." NBS-NSRDS 35, National Bureau of Standards, Washington, DC, 1948.

Table B-2. Coefficients for the Computation of the Thermodynamic Properties of C^{++}

Coefficients	298.15 – 1,000 K	1,000 – 6,000 K	6,000 – 20,000 K
a_1	2.5	2.52243896E+04	1.20211947E+08
a_2	0.0	-7.51998881E+01	-9.04691343E+04
a_3	0.0	2.58833405E+00	2.91778474E+01
a_4	0.0	-5.23213535E-05	-3.85733714E-03
a_5	0.0	1.65224996E-08	2.75797361E-07
a_6	0.0	-2.65014198E-12	-8.55590514E-12
a_7	0.0	1.697303213E-16	9.89664769E-17
b_1	4.9917012E+05	4.99647751E+05	1.19820991E+06
b_2	2.5645969	1.93672086	-2.24190892E+02

NO. OF COPIES ORGANIZATION

2 DEFENSE TECHNICAL INFORMATION CENTER
DTIC DDA
8725 JOHN J KINGMAN RD
STE 0944
FT BELVOIR VA 22060-6218

1 HQDA
DAMO FDQ
D SCHMIDT
400 ARMY PENTAGON
WASHINGTON DC 20310-0460

1 OSD
OUSD(A&T)/ODDDR&E(R)
R J TREW
THE PENTAGON
WASHINGTON DC 20301-7100

1 DPTY CG FOR RDA
US ARMY MATERIEL CMD
AMCRDA
5001 EISENHOWER AVE
ALEXANDRIA VA 22333-0001

1 INST FOR ADVNCD TCHNLGY
THE UNIV OF TEXAS AT AUSTIN
PO BOX 202797
AUSTIN TX 78720-2797

1 DARPA
B KASPAR
3701 N FAIRFAX DR
ARLINGTON VA 22203-1714

1 NAVAL SURFACE WARFARE CTR
CODE B07 J PENNELLA
17320 DAHLGREN RD
BLDG 1470 RM 1101
DAHLGREN VA 22448-5100

1 US MILITARY ACADEMY
MATH SCI CTR OF EXCELLENCE
DEPT OF MATHEMATICAL SCI
MADN MATH
THAYER HALL
WEST POINT NY 10996-1786

NO. OF COPIES ORGANIZATION

1 DIRECTOR
US ARMY RESEARCH LAB
AMSRL DD
2800 POWDER MILL RD
ADELPHI MD 20783-1197

1 DIRECTOR
US ARMY RESEARCH LAB
AMSRL CS AS (RECORDS MGMT)
2800 POWDER MILL RD
ADELPHI MD 20783-1145

3 DIRECTOR
US ARMY RESEARCH LAB
AMSRL CI LL
2800 POWDER MILL RD
ADELPHI MD 20783-1145

ABERDEEN PROVING GROUND

4 DIR USARL
AMSRL CI LP (BLDG 305)

NO. OF
COPIES ORGANIZATION

ABERDEEN PROVING GROUND

26 DIR USARL
AMSRL WM B
A W HORST
AMSRL WM BD
B E FORCH
W R ANDERSON
R A BEYER
S W BUNTE
C F CHABALOWSKI
A COHEN
R DANIEL
D DEVYNCK
R A FIFER
B E HOMAN
A JUHASZ
A J KOTLAR
K L MCNESBY
M MCQUAID (2 CPS)
M S MILLER
A W MIZIOLEK
J B MORRIS
R A PESCE-RODRIGUEZ
B M RICE
R C SAUSA
M A SCHROEDER
J A VANDERHOFF
AMSRL WM BE
M NUSCA (2 CPS)

REPORT DOCUMENTATION PAGE

Form Approved
OMB No. 0704-0188

1. AGENCY USE ONLY *(Leave blank)*	2. REPORT DATE	3. REPORT TYPE AND DATES COVERED
	September 1999	Final, Jan 99 - Jun 99

4. TITLE AND SUBTITLE
Calculating the Chemical Compositions of Plasmas Generated by an Ablating-Capillary Arc

5. FUNDING NUMBERS
622618AH80

6. AUTHOR(S)
M. J. McQuaid and M. J. Nusca

7. PERFORMING ORGANIZATION NAME(S) AND ADDRESS(ES)
U.S. Army Research Laboratory
ATTN: AMSRL-WM-BD
Aberdeen Proving Ground, MD 21005-5066

8. PERFORMING ORGANIZATION REPORT NUMBER
ARL-TR-2046

9. SPONSORING/MONITORING AGENCY NAMES(S) AND ADDRESS(ES)

10.SPONSORING/MONITORING AGENCY REPORT NUMBER

11. SUPPLEMENTARY NOTES

12a. DISTRIBUTION/AVAILABILITY STATEMENT
Approved for public release; distribution is unlimited.

12b. DISTRIBUTION CODE

13. ABSTRACT *(Maximum 200 words)*

The NASA-Lewis computer program for the calculation of complex chemical equilibrium compositions (CEA) is proposed as a means of characterizing the compositions of plasmas generated via an ablating-capillary arc. Results obtained with CEA are compared to those obtained with a Saha equation-based (SE) model with a limited reaction product set. Case studies conducted at temperatures from 5,000 to 20,000 K and pressures from 10 to 200 bar indicate that CEA warrants consideration for use in modeling such plasmas.

14. SUBJECT TERMS
electrothermal-chemical ignition; plasma compositions; ablating-capillary arc

15. NUMBER OF PAGES
43

16. PRICE CODE

17. SECURITY CLASSIFICATION OF REPORT	18. SECURITY CLASSIFICATION OF THIS PAGE	19. SECURITY CLASSIFICATION OF ABSTRACT	20. LIMITATION OF ABSTRACT
UNCLASSIFIED	UNCLASSIFIED	UNCLASSIFIED	UL

INTENTIONALLY LEFT BLANK.

USER EVALUATION SHEET/CHANGE OF ADDRESS

This Laboratory undertakes a continuing effort to improve the quality of the reports it publishes. Your comments/answers to the items/questions below will aid us in our efforts.

1. ARL Report Number/Author ARL-TR-2046 (McQuaid) Date of Report September 1999

2. Date Report Received _____

3. Does this report satisfy a need? (Comment on purpose, related project, or other area of interest for which the report will be used.) _____

4. Specifically, how is the report being used? (Information source, design data, procedure, source of ideas, etc.) _____

5. Has the information in this report led to any quantitative savings as far as man-hours or dollars saved, operating costs avoided, or efficiencies achieved, etc? If so, please elaborate. _____

6. General Comments. What do you think should be changed to improve future reports? (Indicate changes to organization, technical content, format, etc.) _____

CURRENT ADDRESS

Organization

Name E-mail Name

Street or P.O. Box No.

City, State, Zip Code

7. If indicating a Change of Address or Address Correction, please provide the Current or Correct address above and the Old or Incorrect address below.

OLD ADDRESS

Organization

Name

Street or P.O. Box No.

City, State, Zip Code

(Remove this sheet, fold as indicated, tape closed, and mail.)

(DO NOT STAPLE)

DEPARTMENT OF THE ARMY

OFFICIAL BUSINESS

NO POSTAGE
NECESSARY
IF MAILED
IN THE
UNITED STATES

BUSINESS REPLY MAIL
FIRST CLASS PERMIT NO 0001,APG,MD

POSTAGE WILL BE PAID BY ADDRESSEE

DIRECTOR
US ARMY RESEARCH LABORATORY
ATTN AMSRL WM BD
ABERDEEN PROVING GROUND MD 21005-5066